

Impact of on-line calibration of radar-measured rainfall in hydrological forecasting using a distributed hydrological model

MINJIAO LU & NORIO HAYAKAWA

*Department of Civil and Environmental Engineering, Nagaoka University of Technology,
Nagaoka, Niigata 940-2188, Japan*

lu@nagaokaut.ac.jp

Abstract In order to find a more effective way to use both gauge- and radar-measured rainfall data in hydrological forecasting, a runoff analysis was carried out over the Uono River basin (355 km²), a tributary of the Shinano River. A distributed hydrological model was constructed by using our distributed hydrological modelling system. The study basin was divided into small grid cells. This model computes runoff generated in all grid cells from rainfall data using the XinAnJiang model, and routes the runoff from these cells to the basin outlet through a channel network delineated from geographical information. In a discussion on estimation of radar constants, the necessity of on-line calibration of radar rainfall was shown, and an on-line calibration algorithm was developed. Comparing with hydrographs calculated from gauge rainfall, the hydrographs from calibrated radar rainfall showed significant improvement in both cases, peak flows calculated from gauge rainfall were overestimated or underestimated.

Key words distributed hydrological model; hydrological forecasting; on-line calibration; radar hydrology; radar-measured rainfall

INTRODUCTION

Weather radar has been considered to be a powerful tool to provide rainfall data to drive hydrological models, especially distributed models. The high spatial and temporal resolution, and large areal coverage makes it potentially possible to take into account the effects of spatial distribution of rainfall, and to make hydrological forecasting for small and/or ungauged catchments. Up to now, many hydrologists applied and tested the radar rainfall in various hydrological models (Fortin *et al.*, 1986; Kouwen, 1988; Kouwen & Garland, 1989; Lu *et al.*, 1989; Carpenter *et al.*, 2001; Borga, 2002). It has been recognized that radar rainfall uncertainty largely limits its applicability. Krajewski & Georgakakos (1985) showed that error of radar rainfall could be as large as about 50%. This uncertainty makes the spatial averaging necessary (Kouwen & Garland, 1989), and then hinders its application to hydrological forecasting for small and/or ungauged catchments where the advantage of radar rainfall data are considered most significant.

In our previous work (Lu *et al.*, 1996b), it was found that calibration of radar rainfall with gauge-measured basin-average rainfall improves the accuracy of hydrological forecasting. In this study, an investigation of the variability of radar constants was carried out. Their large variability and dependency on the objective functions of optimization methods, and then the necessity of on-line calibration are

shown. The purpose of this work was to develop a methodology of on-line calibration of radar rainfall and complementary use of radar rainfall and gauge rainfall, and to show its impacts on hydrological forecasting. By using this newly developed method, calculated hydrographs are significantly improved for cases where peak flows calculated from gauge rainfall are overestimated or underestimated.

STUDY BASIN AND DATA

The study area is upstream part of the Uono River basin, a tributary of the Shinano River, the longest river in Japan. Its drainage area is 355 km², and the basin discharge is gauged at the outlet (Fig. 1). This basin is hilly with elevation ranging from 100 m to about 2000 m. Figure 1 also shows the polar coordinate system of the Yakushidake weather radar and ten raingauge stations among 16 stations used to calibrate the radar rainfall data. Our study basin was completely covered by this weather radar, which was installed exclusively for rainfall observation. The limit for quantitative observation of this radar is 120 km, and the spatial and temporal resolutions of this radar are 3 km and 5 min, respectively. Though 5-min radar rainfall data are available, the hourly rainfall data are used in this analysis because the conventional data of rainfall and stream flow are collected hourly.

In this basin, floods are mainly caused by frontal storm, thunderstorm, typhoon, cyclone and snowmelt. Heavy frontal storms with a thunderstorm can be observed frequently in summer. A total of 16 flood events shown in Table 1 are selected to

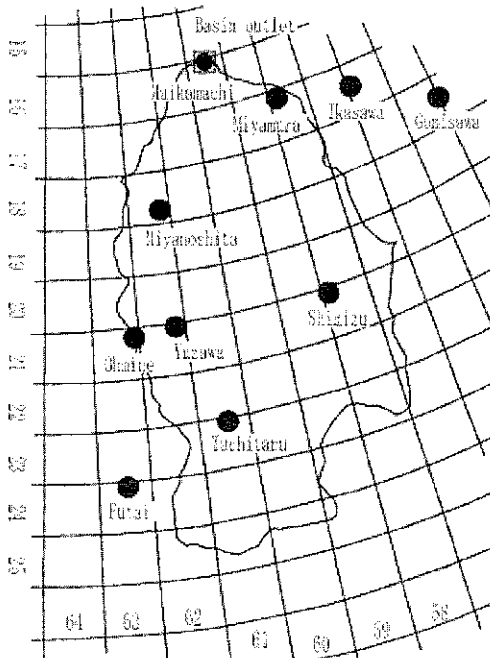


Fig. 1 Study basin.

Table 1 Selected flood events.

Flood no.	Period	Max. rainfall (mm h ⁻¹)	Peak flow (m ³ s ⁻¹)	Time lag (h)	Cause
880824	1988/08/24–08/28	28.2	165.7	2	thunderstorm
880902	1988/09/02–09/04	13.0	195.0	4	thunderstorm
890525	1989/05/25–05/27	10.9	256.5	5	cyclone/front
890806	1989/08/06–08/07	10.6	286.5	4	typhoon
890826	1989/08/26–08/28	12.0	160.0	4	thunderstorm
890904	1989/09/04–09/06	12.1	201.6	4	cyclone/front
890918	1989/09/18–09/21	11.4	222.8	3	typhoon
900919	1990/09/19–09/21	13.9	387.1	2	typhoon
901007	1990/10/07–10/09	13.2	279.9	5	typhoon
901026	1990/10/26–10/28	8.2	195.2	3	cyclone/front
910830	1991/08/30–09/01	21.9	714.7	2	typhoon
911012	1991/10/12–10/14	5.2	33.5	5	typhoon
930826	1993/08/26–08/27	9.0	224.8	4	typhoon
940929	1994/09/29–10/01	9.4	381.5	3	typhoon
950708	1995/07/08–07/24	15.5	189.4	4	meiyu front
950915	1995/09/15–09/18	9.5	158.6	5	typhoon

investigate the possibility of using radar-measured rainfall in hydrological forecasting. Among them, three are caused by thunderstorms, nine by typhoons, three by cyclones and/or fronts, and one by a meiyu front. All causes of flood events in this area, except snowmelt, are considered.

DISTRIBUTED HYDROLOGICAL MODEL

A distributed hydrological model developed by Lu *et al.* (1996a) was used. The study basin was then divided into small grid cells. From field surveys and the result of distributed snowmelt analysis, we found that the hydrological processes can be classified into two groups: the processes within a grid cell and those between grid cells when the grid spacing is as large as several hundred metres. The processes within a grid cell can be simulated grid cell by grid cell, and the interaction between grid cells is assumed not to be dominant. The movement of water between grid cells is simulated by our runoff routing model. The runoff of a grid cell is concentrated to its centre and considered to flow to one of its eight neighbours, forming the steepest slope. The flow path between these two grid points (the centre of a grid cell) is modelled as an open channel with a wide rectangular cross-section. The runoff together with inflow from upstream channels is routed to the downstream end of this channel by using a routing scheme. In this model, all channels are arranged into an optimal routing sequence according to the structure of the channel network, which keeps the downstream channel to be routed after its upstream ones (Lu *et al.*, 1996a).

The study basin, the Uono River basin, is divided into 36 233 grid cells of 100 m × 100 m (slightly larger than officially published drainage area 355 km²). From geographical information, a channel network that links all grid cells to the basin outlet

is automatically delineated. At each grid point, the input data are assigned from available data sources, for example gauge rainfall and radar rainfall. Using the assigned rainfall data, runoff is calculated at each grid cell by using a conceptual rainfall-runoff model, the XinAnJiang model (Zhao, 1992), and then routed to the basin outlet through the channel network. In routing computation of each river channel, the kinematic wave approximation is used that considers the hilly topography of this basin. All model parameters are calibrated in previous studies.

ESTIMATION OF RADAR CONSTANTS

The radar rainfall uses the so-called radar equation in which the rainfall intensity is related to the radar reflectivity in the form of a power law given as follows:

$$Z = BR^\beta \quad (1)$$

where B and β are radar constants, which can be determined theoretically under some assumptions. For the Yakushidake radar, $B = 650$ and $\beta = 1.5$ is provided by a hardware company and used operationally (due to a hardware reason, Z and then B are multiplied by a factor of four). However, in most applications of radar rainfall, these constants are fitted with the observed data. Before running the distributed model, we tried to fit these constants for each flood event and for all events by using the following three methods:

(a) Optimize $\ln B$ and β by minimizing the objective function:

$$S(B, \beta) = \frac{1}{N} \sum_s \sum_t (\ln Z_s(t) - \ln B - \beta \ln R_s(t))^2 \quad (2)$$

$$Z_s(t) = \frac{1}{12} \sum_{k=0}^{11} Z_s(t-k/12)$$

where $R_s(t)$ is hourly rainfall in the t th hour observed at the s th gauge station, and $Z_s(t)$ is hourly mean radar reflectivity corresponding to the s th station, N is the number of all effective data. In this study, all data of 16 stations are used.

(b) Optimize a and b by minimizing the objective function:

$$S(a, b) = \frac{1}{N} \sum_s \sum_t (\ln R_s(t) - a \ln Z_s(t) - b)^2 \quad (3)$$

and then obtain radar constants by $\beta = 1/a$ and $B = \exp(-b\beta)$;

(c) Optimize B and β directly by minimizing the objective function:

$$S(B, \beta) = \frac{1}{N} \sum_s \sum_t \left| R_s(t) - \frac{1}{12} \sum_{k=0}^{11} \left(\frac{Z_s(t-k/12)}{B} \right)^{1/\beta} \right| \quad (4)$$

In methods (a) and (b) (referred to as EST(Z) and EST(r)), radar constants can be explicitly obtained from observed gauge rainfall and radar reflectivity data. They, especially EST(Z), are mostly used in estimation of radar constants. Method (c) (referred to as OPT) is obviously a nonlinear optimization problem. Method (c) is

Table 2 Estimated radar constants.

Flood	EST(r)		EST(Z)		OPT	
	B_r	β_r	B_z	β_z	B_o	β_o
880824	693.00	2.074	1893.59	1.133	4062.42	1.004
880902	1631.80	2.077	3433.41	1.119	2644.18	1.389
890525	266.45	3.668	956.34	1.724	1879.76	1.523
890806	58.28	3.925	692.99	1.319	1841.73	1.150
890826	238.72	4.031	696.69	1.793	2297.18	1.294
890904	238.30	4.191	574.00	1.960	399.41	2.215
890918	188.94	3.703	724.23	1.750	200.32	2.757
900919	240.45	3.302	1766.07	1.149	288.92	2.480
901007	86.30	5.350	340.62	1.733	649.64	1.920
901026	409.65	3.101	1096.93	1.802	170.87	2.871
910830	99.22	3.662	766.67	1.475	1120.33	1.617
911012	5.52	7.901	447.29	1.439	0.02	10.376
930826	137.72	2.848	963.67	1.125	13.90	3.726
940929	204.21	4.652	443.17	2.190	2450.67	1.300
950708	292.311	2.708	626.63	1.428	434.59	1.690
950915	272.93	3.372	588.22	1.742	389.36	2.371
All	189.46	3.552	695.26	1.567	442.67	2.158

designed considering minimization of the error of rainfall itself is more important than that of $\ln(Z)$ or $\ln(R)$ in hydrological forecasting. Here, the quasi Newton method (Meza, 1994) is used to solve the nonlinear optimization problem.

Table 2 shows the estimated radar constants. It is shown that the radar constants vary largely from event to event, and from method to method. For flood no. 911012, methods minimizing the error of R or $\ln(R)$ gave extremely small B and extremely large β because the range of value of R is too small to perform such optimization. It is expected that data covering a wider range of R and Z will improve the estimation of radar constants. However, even using all data of 16 flood events, three methods gave largely different radar constants. Figure 2 shows the value of the objective function used in OPT and the estimated radar constants. In this figure, radar constants derived from EST(r) and EST(Z) are also plotted. From a viewpoint of water balance, it is very hard to say the results of EST(r) and EST(Z) are optimal. Figure 3 shows the accumulated basin-average rainfall of floods no. 880824 and no. 890806. Besides gauge-measured rainfall data, rainfall estimation using operational radar constants (referred to as OPE) and radar constants estimated by EST(r), EST(Z), and OPT are also plotted. Including these two flood events, EST(Z) overestimates and EST(r) underestimates the basin-average rainfall for all 16 flood events. OPT gave values closest to the gauge measured basin-average rainfall. This implies that selection of objective function is also an important issue in application of radar rainfall.

ON-LINE CALIBRATION OF RADAR-MEASURED RAINFALL

Because of the large variability of radar constants, we decided to use operational radar constants to estimate radar rainfall, and then make on-line calibration. For each grid

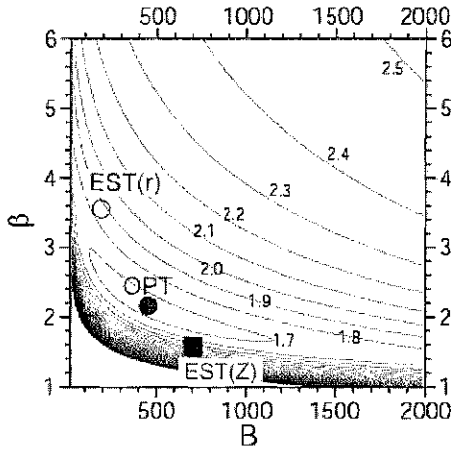


Fig. 2 Mean absolute error of radar rainfall.

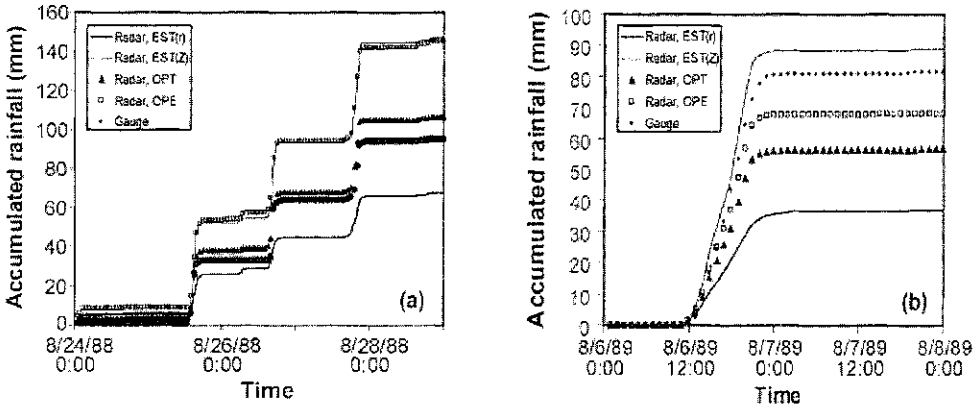


Fig. 3 Accumulated basin-average rainfall: (a) flood no. 880824; (b) flood no. 890806.

cell (i, j) , the composite rainfall $r(i, j, t)$ is assigned as follows:

$$r(i, j, t) = \exp(-l/L)r_c(i, j, t) + (1 - \exp(-l/L))r_r(i, j, t) \tag{5}$$

$$r_c(i, j, t) = G(i, j)r_g(i, j, t) = \frac{\sum_{m=0}^{\infty} k^m r_g(i, j, t-m)}{\sum_{m=0}^{\infty} k^m r_r(i, j, t-m)} r_r(i, j, t) \tag{6}$$

where t represents time, l is distance from grid cell (i, j) to nearest gauge station, $r_g(i, j, t)$ is rainfall data at the nearest gauge station, $r_r(i, j, t)$ is radar rainfall at the radar grid cell covering grid cell (i, j) , k and L are parameters. $r_c(i, j, t)$ is radar rainfall calibrated by using gauge rainfall at the nearest gauge station. When the value of k increases, the antecedent rainfall will have more contribution on the calibration, and

ratio $G(i,j)$ will become more stable. In a sensitivity analysis, it is found that k does not largely affect the calibrated rainfall, which is quite near to the gauge rainfall. In this study, $k = 0.5$ is used. As shown in equation (5), composite rainfall $r(i,j,t)$ consists of two parts, calibrated radar rainfall and raw radar rainfall. The nearer the grid cell (i,j) to a gauge station, the more the calibrated radar rainfall contributes. This allows us to use more information from gauge rainfall for a basin with a dense network of gauge stations, and more information from radar rainfall for a basin with a sparse network of gauge stations.

Using composite rainfall, hydrographs at the basin outlet are derived from our distributed hydrological model. Figure 4 shows the results for floods no. 880824 and no. 890806. In this figure, hydrographs derived by using gauge rainfall, radar rainfall, composite rainfall with different L are plotted. For flood no. 880824 (Fig. 4(a)), the third peak of discharge reproduced by gauge rainfall and radar rainfall is

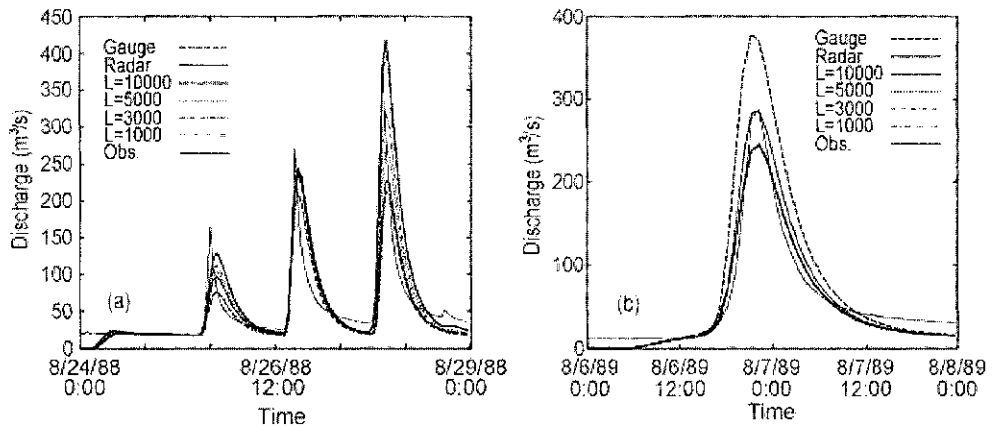


Fig. 4 Observed and calculated hydrographs: (a) flood no. 880824; (b) flood no. 890806.

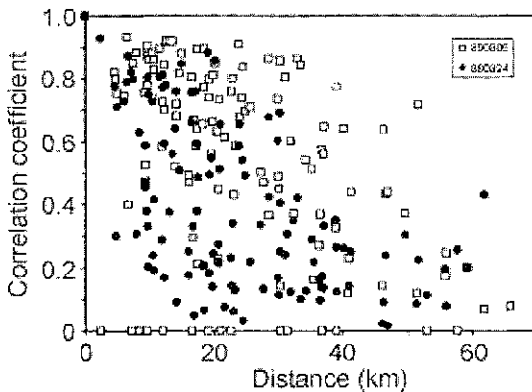


Fig. 5 Relationship between correlation coefficient of rainfall and distance of any two raingages.

underestimated and overestimated, respectively, and the use of composite rainfall with $L = 1000\text{--}3000$ m significantly improves the representation of peak flow. In contrast, for flood no. 890806 (Fig. 4(b)) the peak flow reproduced by gauge rainfall and radar rainfall is overestimated and underestimated, respectively, and the use of composite rainfall with $L = 10\,000$ m improves the representation of the peak flow. Parameter L seems to have a relationship with the spatial scale of the storm. Flood no. 880824 is caused by a thunderstorm with smaller spatial scale while flood no. 890806 is caused by a typhoon with larger scale. Figure 5 shows the relationship between the rainfall correlation coefficient and distance of any two gauge stations. Obviously, the correlation coefficient of rainfall decreases more slowly when the distance becomes larger for flood no. 890806, due to its larger spatial scale.

CONCLUSIONS

Three methods are used to estimate radar constants for each flood event. It is shown that the estimated radar constants change from event to event, and from method to method. Even using all data of 16 flood events, the radar constants estimated by the three methods are quite different. Radar constants estimated by minimizing RMS error of $\ln(Z)$ are the nearest to the operational radar constants. However, they differ from those estimated by minimizing RMS error of $\ln(R)$ or mean absolute error of rainfall. From the viewpoint of water balance, minimization of error of rainfall itself is an important issue. The mean absolute error shows that the method minimizing RMS error of $\ln(R)$ or RMS error of $\ln(Z)$ can hardly be considered as optimal.

Because of the large variability of the estimated radar constants, we decided to use operational radar constants and to make complementary use of gauge rainfall and radar rainfall. A new methodology of on-line calibration was developed. It was shown that significant improvements are achieved by using this method in cases where peak flows calculated from gauge rainfall are overestimated or underestimated. Also, the dependency of parameters of this method on the spatial scale of rainfall is clarified. Further work on this issue will be carried out to make this method applicable to operational hydrological forecasting.

Acknowledgements In this study, the Object-Oriented Nonlinear Optimization Library at the OPT++ developed in Sandia National Laboratories, Livermore, California, USA was used.

REFERENCES

- Borga, M. (2002) Accuracy of radar rainfall estimates for streamflow simulation. *J. Hydrol.* **267**, 26–39.
- Carpenter, T. M., Georgakakos, K. P. & Sperflage J. A. (2001) On the parametric and NEXRAD-radar sensitivities of a distributed hydrologic model suitable for operational use. *J. Hydrol.* **253**, 169–193.
- Fortin, J. P., Villeneuve, J. P., Guilbot, A. & Seguin, B. (1986) Development of a modular hydrological forecasting model based on remotely sensed data, for interactive utilization on a microcomputer. In: *Hydrologic Applications of Space Technology* (ed. by A. I. Johnson) (Proc. Workshop, August 1985), 307–319. IAHS Publ. no. 160.
- Kouwen, N. (1988) Watflood: a micro-computer based flood forecasting system based on real-time weather radar. *Can. Water Resour. J.* **13**(1), 62–77.

- Kouwen, N. & Garland G. (1989) Resolution considerations in using radar rainfall data for flood forecasting. *Can. J. Civil Engng* **16**, 279–289.
- Krajewski, W. F. & Georgakakos, K. P. (1985) Synthesis of radar rainfall data. *Water Resour. Res.* **21**, 746–768.
- Lu, M., Koike, T. & Hayakawa, N. (1989) A rainfall–runoff model using distributed data of radar rain and altitude. *J. Hydraul. Coastal & Environ. Engng* **411**(11–12), 135–140.
- Lu, M., Koike, T. & Hayakawa, N. (1996a) A distributed hydrological modelling system linking GIS and hydrological models. In: *Application of Geographic Information Systems in Hydrology and Water* (ed. by K. Kovar & H. P. Nachtnebel) (Proc. HydroGIS'96 Conf.), 141–148. IAHS Publ. no. 235.
- Lu, M., Koike, T. & Hayakawa, N. (1996b) Distributed XinAnJiang model using radar measured rainfall data. In: *Water Resources & Environmental Research: Towards the 21st Century* (Proc. Int. Conf.), **1**, 29–36.
- Meza, J. C. (1994) OPT++: An object-oriented class library for nonlinear optimization. Sandia Tech. Report no. SAND94-8225, Sandia National Laboratories, Livermore, California, USA.
- Zhao, R.-J. (1992) The XinAnJiang model applied in China. *J. Hydrol.* **135**, 371–381.